ELSEVIER

SCIENCE DIRECT®

PHYSICS LETTERS B

Physics Letters B 587 (2004) 52–61

www.elsevier.com/locate/physletb

Nuclear shadowing in neutrino–nucleus deeply inelastic scattering

Jianwei Qiu, Ivan Vitev

Department of Physics and Astronomy, Iowa State University, Ames, IA 50011, USA

Received 12 February 2004; accepted 28 February 2004

Editor: H. Georgi

Abstract

In the framework of the collinear factorized pQCD approach we calculate the small-x_B process-dependent nuclear modification to the structure functions measured in neutrino–nucleus deeply inelastic scattering. We include both heavy quark mass corrections (M^2/Q^2) and resummed nuclear-enhanced dynamical power corrections in the quantity $(\xi^2/Q^2)(A^{1/3}-1)$ with ξ^2 evaluated to leading order in α_s. Our formalism predicts a measurable difference in the shadowing pattern of the structure functions $F_2^A(x_B,Q^2)$ and $F_3^A(x_B,Q^2)$ and a significant low- and moderate-Q^2 modification of the QCD sum rules. We also comment on the relevance of our results to the NuTeV extraction of $\sin^2\theta_W$.

PACS: 12.38.Cy; 12.39.St; 24.85.+p; 25.30.-c

1. Introduction

Recent surprising results on $\sin^2\theta_W$, reported by the NuTeV Collaboration and based on a comparison of charged and neutral current neutrino interactions with an iron rich target [1], renewed our quest for understanding the nuclear dependence in neutrino–nucleus deeply inelastic scattering (DIS). A possibility that process-dependent nuclear shadowing might affect the NuTeV extraction of the Weinberg angle θ_W was raised by Miller and Thomas [2]. Although such scenario was considered unlikely by the Collaboration [3], a systematic study and a clear understanding of the process-dependent nuclear effects in neutrino–nucleus scattering will strengthen the importance of the NuTeV result.

Like all nuclear dependences in the physical cross sections [4], the small-x_B shadowing in lepton–nucleus DIS has both process-dependent and process-independent contributions. While its universal part can be factorized in the leading twist nuclear parton distribution functions (nPDFs), the DIS-specific modifications arise from the higher twist (or power) corrections to the structure functions [2,5,6]. In this Letter, we present a calculation of the process-dependent shadowing in neutrino–nucleus deeply inelastic scattering by resumming heavy quark mass corrections, $M^2/(2p\cdot q)=x_B M^2/Q^2$, and nuclear size enhanced dynamical power corrections, $(\xi^2/Q^2)(A^{1/3}-1)$ with $\xi^2\propto\langle F^{+\perp}F^{+}_{\perp}\rangle$, the gluon density in a large nucleus. The numerical value for the characteristic scale of higher twist

E-mail address: jwq@iastate.edu (J. Qiu).

doi:10.1016/j.physletb.2004.02.065

ξ^2 [6], extracted from DIS data on μ–A interactions [7], is much less than Q^2 in the region which is perturbatively accessible. Therefore, we only evaluate ξ^2 to the leading order in α_s, while resumming the power corrections to all orders in $(\xi^2/Q^2)(A^{1/3}-1)$. Using $\xi^2 = 0.09$–$0.12\ \mathrm{GeV}^2$ [6], our results provide a good description of the deviation between the Gross–Llewellyn Smith QCD sum rule [8] adjusted for $\mathcal{O}(\alpha_s)$ scaling violations [9] and the existing data [10]. At small Bjorken x_B, the high twist components to the calculated structure functions $F_2^A(x_B, Q^2)$ and $F_3^A(x_B, Q^2)$ in neutrino-iron DIS qualitatively describe the low-x_B and low-Q^2 suppression trend in the preliminary data, recently reported by the NuTeV Collaboration at DIS 2003 [11].

In the next section we briefly review the DIS kinematics and coherence at small Bjorken x_B. In Section 3 we demonstrate that at the tree level mass corrections and dynamical power corrections "commute" and their resummation can be carried out in a closed form. We derive analytic expressions for the process-dependent nuclear modification to the transverse and longitudinal structure functions in neutrino–nucleus DIS. In Section 4 we predict the difference in the shadowing pattern of $F_2^A(x_B, Q^2)$ and $F_3^A(x_B, Q^2)$, and give quantitative results for the x_B-, A- and Q^2-dependence of the nuclear modification to the charged current $\nu(\bar{\nu})$-A DIS structure functions. We find sizable small- and moderate-Q^2 corrections to the Gross–Llewellyn Smith QCD sum rule. In Section 5 we comment on the relevance of our results to the NuTeV extraction of $\sin^2\theta_W$. Finally, we give our conclusions in Section 6.

2. DIS kinematics and coherence at small x_B

The charged current DIS cross section of a neutrino (or antineutrino) beam (k) off a nuclear target (P_A), as illustrated in Fig. 1(a), probes three independent structure functions, $F_i^A(x_B, Q^2)$ with $i = 1, 2, 3$ [9]

$$\frac{d\sigma^{\nu(\bar{\nu})A}}{dx_B\,dy} = \frac{\pi\alpha_{\mathrm{em}}^2 m_N E}{2\sin^4(\theta_W)(Q^2+M_W^2)^2}\left[\frac{y^2}{2}2x_B F_1^{\nu(\bar{\nu})A} + \left(1 - y - y\frac{m_N x_B}{2E}\right)F_2^{\nu(\bar{\nu})A} + (-)\left(y - \frac{y^2}{2}\right)x_B F_3^{\nu(\bar{\nu})A}\right], \tag{1}$$

where the Bjorken variable $x_B = Q^2/(2p\cdot q)$ with $p = P_A/A$, the exchanged W-boson momentum is q and its virtuality $Q^2 = -q^2$, and $y = p\cdot q/(p\cdot k)$. In Eq. (1), the '$(-)$' represents the sign for an antineutrino beam, $m_N = M_A/A$ with nuclear mass M_A, M_W is the W-boson mass, and E is the beam energy. The often-referred longitudinal structure function, $F_L^{\nu(\bar{\nu})A} = F_2^{\nu(\bar{\nu})A}/(2x_B) - F_1^{\nu(\bar{\nu})A}$ if $4x_B^2 m_N^2 \ll Q^2$ [9]. Here, we are predominantly interest in the small-x_B region and neglect the target mass (rescaling) corrections [12].

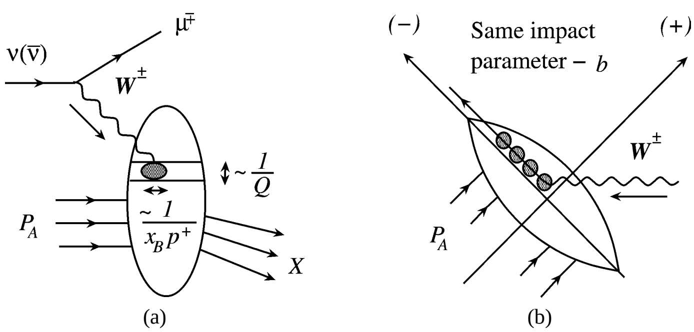

Fig. 1. (a) Illustration of the characteristic scales, $A_\perp = 1/Q^2$ and $\Delta z^{(-)} = 1/(x_B p^+)$ in the boosted frame, probed by the virtual meson in DIS. (b) Multiple final state interactions of the struck quark with the partons from the nucleus at a fixed impact parameter b.

The DIS cross section with an exchange of a W- or Z-boson of virtuality Q^2 and energy $\nu = Q^2/(2m_N x_B)$ has an effective resolution in transverse area $A_\perp = 1/Q^2$, which is much less than the nucleon size, and an uncertainty in longitudinal direction $\Delta z^{(-)} = 1/(x_B p^+)$ with boosted nucleon momentum p^+. If $\Delta z^{(-)} = 1/(x_B p^+) \geqslant 2r_0(m_N/p^+)$ or $x_B \leqslant x_N = 1/(2m_N r_0) \sim 0.1$, the neutrino will *coherently* interact with more than one nucleon inside the nucleus, and probe the nuclear dependence at a perturbative scale Q^2 [5,6,13].

3. Calculating mass and dynamical power corrections

Electroweak charged and neutral current processes necessitate a discussion of final state charm mass effects in neutrino–nucleus DIS even if the leading twist charm quark parton distribution is neglected, $\phi_c(x, Q^2) = \phi_{\bar{c}}(x, Q^2) = 0$ [14]. It is, therefore, critical to develop a systematic approach to the interplay of a heavy quark final state and the resummed nuclear enhanced power corrections discussed in [6]. We define the boost invariant mass fraction

$$x_M = \frac{M^2}{2p\cdot q} = x_B \frac{M^2}{Q^2} \tag{2}$$

and choose a frame such that $p^\mu = p^+ \bar{n}^\mu$ and $q^\mu = -x_B p^+ \bar{n}^\mu + Q^2/(2x_B p^+) n^\mu$, where $\bar{n}^\mu = [1, 0, 0_\perp]$ and $n^\mu = [0, 1, 0_\perp]$ specify the '+' and '−' lightcone directions, respectively. With a non-vanishing quark mass M, the Feynman rule for the final state cut line of quark momentum $x_i p + q$ in Fig. 2(a) is

$$\mathrm{Cut} = 2\pi \left(\frac{x_B}{Q^2}\right)(\gamma\cdot\tilde{p} + M)\delta(x_i - x_B - x_M), \tag{3}$$

where

$$\tilde{p}^\mu = x_M p^+ \bar{n}^\mu + \frac{Q^2}{2x_B p^+} n^\mu, \tag{4}$$

with $\tilde{p}^2 = M^2$. For $M \to 0$ we recover the known massless case, in which the scattered quark is moving along the '−' lightcone direction. A direct consequence of this Feynman rule is a tree-level coupling for longitudinally polarized vector mesons $\propto M^2/Q^2$. Contracting $\epsilon_L^{\mu\nu}$ [15] with the charged current hadronic tensor $W_{\mu\nu}$ [9] yields:

$$\frac{1}{A} F_L^{\nu A}\big(x_B, Q^2\big) = \sum_{D,U} |V_{DU}|^2 \frac{M_U^2}{Q^2} \phi_D^A\big(x_B + x_{M_U}, Q^2\big) + \sum_{\bar{U},\bar{D}} |V_{\bar{U}\bar{D}}|^2 \frac{M_{\bar{D}}^2}{Q^2} \phi_{\bar{U}}^A\big(x_B + x_{M_{\bar{D}}}, Q^2\big), \tag{5}$$

$$\frac{1}{A} F_L^{\bar{\nu} A}\big(x_B, Q^2\big) = \sum_{U,D} |V_{UD}|^2 \frac{M_D^2}{Q^2} \phi_U^A\big(x_B + x_{M_D}, Q^2\big) + \sum_{\bar{D},\bar{U}} |V_{\bar{D}\bar{U}}|^2 \frac{M_{\bar{U}}^2}{Q^2} \phi_{\bar{D}}^A\big(x_B + x_{M_{\bar{U}}}, Q^2\big), \tag{6}$$

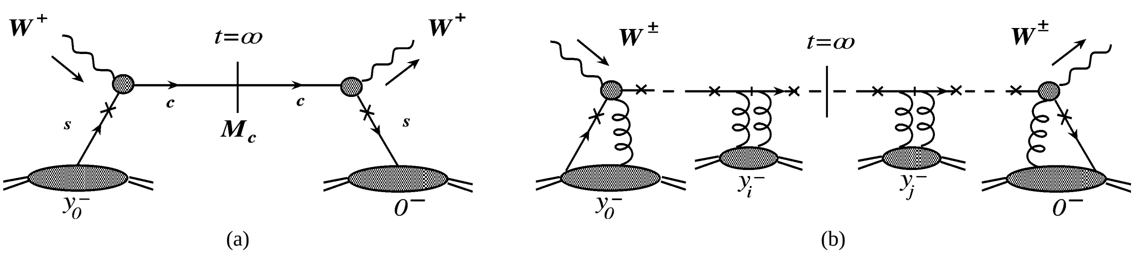

Fig. 2. (a) Tree level direct coupling of the exchange vector meson $W^\pm$ to the struck quark in charge current neutrino–nucleus DIS with massive charm final state. (b) Tree-level contribution to the nuclear-enhanced dynamical power corrections with heavy quark effects.

where the CKM matrix elements V_{ij} parametrize the electroweak and mass eigenstate mixing with up-type quark $U=(u,c,t)$ and down-type quark $D=(d,s,b)$ [9], and ϕ_i^A represent the flavor-i universal twist-2 parton distribution functions (PDFs) of a nucleon ($A=1$) or a nucleus [5]. Eqs. (5) and (6) give a novel leading order (α_s^0) power suppressed (M^2/Q^2) quark mass contribution to the ratio of longitudinal and transverse structure functions $R(x_B,Q^2)=F_L^A(x_B,Q^2)/F_1^A(x_B,Q^2)$ for both nucleons and nuclei.

We calculate the nuclear enhanced dynamical power corrections in the lightcone $A^+=0$ gauge. In this gauge, other than the initial-state contact-term contributions, all leading order nuclear enhanced power corrections are from final-state multiple gluon interactions of the scattered quark in a large nucleus shown in Fig. 2(b) [6]. To resum all order nuclear enhanced power corrections with a non-vanishing (anti)quark mass, we examine its propagator structure [16]. For a quark momentum $x_i p+q$

$$\text{Propagator}=\pm i\left(\frac{x_B}{Q^2}\right)\gamma\cdot p\pm i\left(\frac{x_B}{Q^2}\right)\frac{\gamma\cdot\tilde p+M}{x_i-(x_B+x_M)\pm i\epsilon}, \tag{7}$$

where $\pm i, \pm i\epsilon$ correspond to propagators to the left or right of the $t=\infty$ cut. In the Fourier space conjugate to $x_i p^+$ the first term, free of x_i pole, is $\propto\delta(y_i^-)$. The operators in the hadronic matrix element that this contact term ($\not\to$) separates can be evaluated in the same nucleon state [6]. In contrast, the Fourier transform of the second term is $\propto\theta(y_i^-)$. Therefore, this pole term ($\not\to\!\!\to$) is the source of the $A^{1/3}$ nuclear size enhancement to the power corrections. The operators that it connects in the multi-field multi-local hadronic matrix element can be long-distance separated and thus approximately evaluated in different nucleon states [6]. Alternative operator decompositions as well as other terms that arise from a formal operator product expansion (OPE) [17] are suppressed by powers of the nuclear size.

The case of massive final state quarks could be much more involved than the $M\to 0$ limit. The complexity of the calculation stems from the potentially dangerous exponential growth of the number of terms coming from products of propagators, see Fig. 2(b). In our calculation we first observe that $\gamma\cdot\tilde p+M$ in the cut line, Eq. (3), and the numerator of the pole-term, Eq. (7), arise from an *on-shell* momentum $\tilde p$. Since the exchange gluons at the vertices connected by quark propagators are transversely polarized in the $A^+=0$ physical gauge, $A_\mu(y_i^-)\gamma^\mu\approx A_\perp(y_i^-)\gamma^\perp$,

$$\cdots\gamma\cdot p\gamma^\perp\gamma\cdot p\cdots\propto -p^2\gamma^\perp=0,$$
$$\cdots(\gamma\cdot\tilde p+M)\gamma^\perp(\gamma\cdot\tilde p+M)\cdots\propto-\big(\tilde p^2-M^2\big)\gamma^\perp=0.$$

For the diagrams in Fig. 2(b) only one *alternating* sequence of short and long distance parts of the propagators Eq. (7), initiated by the $t=\infty$ cut, survives. Therefore, there must be an *even* number of gluon interactions between the cut line and any surviving pole term of a propagator in Fig. 2(b). We also note that

$$\cdots\gamma\cdot p(\gamma\cdot\tilde p\pm M)\gamma\cdot p\cdots\propto\gamma^-p^+\left(\frac{Q^2}{2x_Bp^+}\gamma^+\right)\gamma^-p^+$$

leaves no mass dependence in the spinor trace of the diagrams. The basic unit for two-gluon exchange with a net momentum fraction flow x_i-x_{i-1} and two-quark-propagators (one contact plus one pole) [6], see Fig. 2(b), now reads:

$$\text{Unit}=x_B\left(\frac{4\pi^2\alpha_s}{3Q^2}\right)\int\frac{d\lambda_i}{2\pi}\frac{e^{i(x_i-x_{i-1})\lambda_i}}{x_i-x_{i-1}-i\epsilon}\begin{cases}\frac{\gamma^-\gamma^+}{2}\frac{-i\hat F^2(\lambda_i)}{x_{i-1}-(x_B+x_M)+i\epsilon}, & \text{left},\\ \frac{\gamma^+\gamma^-}{2}\frac{-i\hat F^2(\lambda_i)}{x_i-(x_B+x_M)-i\epsilon}, & \text{right}.\end{cases} \tag{8}$$

In Eq. (8) the boost invariant $\lambda_i=p^+y_i^-$, the two cases correspond to a vertex to the left or right of the final state cut and $\hat F^2(\lambda_i)$ is given by the intra-nucleon two-gluon field strength correlator defined in [6]:

$$\hat F^2(\lambda_i)\equiv\int\frac{d\tilde\lambda_i}{2\pi}\frac{1}{(p^+)^2}F^{+\alpha}(\lambda_i)F_\alpha^{+}(\tilde\lambda_i)\theta(\lambda_i-\tilde\lambda_i). \tag{9}$$

We conclude that the dynamical nuclear-enhanced all twist contributions from the leading order in α_s Feynman diagrams with a massive quark final state are identical to the massless case up to the substitution $x_B \to x_B + x_M$ (rescaling) in the δ-function in the cut, Eq. (3), and the propagator poles, Eq. (8). Effectively, we have shown that the mass and nuclear enhanced power corrections "commute" and $x_i = x_B + x_M$ for all 'i'. This allows us to take all possible final state interaction diagrams and all possible cuts [18] to explicitly carry out the resummation of coherent high-twist contributions to neutrino–nucleus DIS structure functions,

$$\frac{1}{A}F_{1,3}^{\nu A}\big(x_B, Q^2\big) \approx \{2\}\bigg(\sum_{D,U}|V_{DU}|^2\phi_D^A\big(x_B + x_{\mathrm{HT}} + x_{M_U}, Q^2\big) \pm \sum_{\bar U,\bar D}|V_{\bar U\bar D}|^2\phi_{\bar U}^A\big(x_B + x_{\mathrm{HT}} + x_{M_{\bar D}}, Q^2\big)\bigg), \tag{10}$$

$$\frac{1}{A}F_{1,3}^{\bar\nu A}\big(x_B, Q^2\big) \approx \{2\}\bigg(\sum_{U,D}|V_{UD}|^2\phi_U^A\big(x_B + x_{\mathrm{HT}} + x_{M_D}, Q^2\big) \pm \sum_{\bar D,\bar U}|V_{\bar D\bar U}|^2\phi_{\bar D}^A\big(x_B + x_{\mathrm{HT}} + x_{M_{\bar U}}, Q^2\big)\bigg). \tag{11}$$

In Eqs. (10) and (11) the '$\pm$' signs refer to F_1 (parity conserving) and F_3 (parity violating) transverse structure functions, respectively. The factor '{2}' gives the standard normalization for F_3 only [9] and the isospin average in the PDFs over the protons and neutrons in the nucleus is implicit. In Eqs. (10) and (11) x_{HT} is the momentum fraction shift (rescaling) induced by nuclear enhanced dynamical power corrections and derived in Ref. [6]:

$$x_{\mathrm{HT}} = x_B\frac{\xi^2}{Q^2}\big(A^{1/3} - 1\big)f(x_B), \tag{12}$$

where ξ^2 represents the effective scale for the dynamical power corrections. To the leading order in α_s it is given by

$$\xi^2 = \frac{3\pi\alpha_s(Q^2)}{8r_0^2}\langle p|\hat F^2|p\rangle, \tag{13}$$

where $\langle p|\hat F^2|p\rangle$ depends on the small-x limit of the gluon distribution in the nucleon/nucleus [6]. While $x_N \approx 0.1$ is the limiting value for the onset of coherence, at $x_A = 1/(2m_N r_0 A^{1/3}) < x_N$ the exchange vector meson already probes the full nuclear size, see Fig. 1. To first approximation, the function

$$f(x_B) = \begin{cases} 0, & x_B > x_N, \\ \frac{x_B^{-1} - x_N^{-1}}{x_A^{-1} - x_N^{-1}}, & x_A \leqslant x_B \leqslant x_N, \\ 1, & x_B < x_A \end{cases} \tag{14}$$

in Eq. (12) represents the interpolation between the two regimes based on the uncertainty principle [20]. The nuclear enhancement factor $(A^{1/3} - 1)$ in Eq. (12) comes from the integration $\int d\lambda_i$ in Eq. (8), the lower limit of which was chosen such that the effect vanishes for the proton ($A = 1$) case.

Including the dynamical power corrections, the longitudinal structure functions in Eqs. (5) and (6) become:

$$\begin{aligned}\frac{1}{A}F_L^{\nu A}\big(x_B, Q^2\big) \approx{}& F_L^{(\mathrm{LT})}\big(x_B, Q^2\big) + \sum_{D,U}|V_{DU}|^2\bigg[\frac{M_U^2}{Q^2} + \frac{\xi^2}{Q^2}\bigg(2 - \frac{M_U^2}{Q^2 + M_U^2}\bigg)^2\bigg]\phi_D^A\big(x_B + x_{\mathrm{HT}} + x_{M_U}, Q^2\big) \\ &+ \sum_{\bar U,\bar D}|V_{\bar U\bar D}|^2\bigg[\frac{M_{\bar D}^2}{Q^2} + \frac{\xi^2}{Q^2}\bigg(2 - \frac{M_{\bar D}^2}{Q^2 + M_{\bar D}^2}\bigg)^2\bigg]\phi_{\bar U}^A\big(x_B + x_{\mathrm{HT}} + x_{M_{\bar D}}, Q^2\big),\end{aligned} \tag{15}$$

$$\frac{1}{A}F_L^{\bar{\nu}A}(x_B, Q^2) \approx F_L^{(\mathrm{LT})}(x, Q^2) + \sum_{U,D} |V_{UD}|^2 \left[\frac{M_D^2}{Q^2} + \frac{\xi^2}{Q^2}\left(2 - \frac{M_D^2}{Q^2 + M_D^2}\right)^2\right] \phi_U^A(x_B + x_{\mathrm{HT}} + x_{M_D}, Q^2)$$
$$+ \sum_{\bar{D},\bar{U}} |V_{\bar{D}\bar{U}}|^2 \left[\frac{M_{\bar{U}}^2}{Q^2} + \frac{\xi^2}{Q^2}\left(2 - \frac{M_{\bar{U}}^2}{Q^2 + M_{\bar{U}}^2}\right)^2\right] \phi_{\bar{D}}^A(x_B + x_{\mathrm{HT}} + x_{M_{\bar{U}}}, Q^2). \tag{16}$$

In Eqs. (15) and (16) we include the $\mathcal{O}(\alpha_s)$ leading twist longitudinal structure functions $F_L^{(\mathrm{LT})}(x, Q^2)$ [9] since they are of the same order as the leading ξ^2 power. For numerical evaluation in the next section we consider two quark generations, $U = (u, c)$ and $D = (d, s)$, and use $|V_{ud}|^2 = |V_{cs}|^2 = \cos^2\theta_c = 0.95$, $|V_{us}|^2 = |V_{cd}|^2 = \sin^2\theta_c = 0.05$ with Cabibbo angle θ_c [19]. The u, d and s quarks are treated as massless and the charm quark mass is set to $M_c = 1.35$ GeV [1].

4. Higher twist, shadowing and QCD sum rules

We first quantify analytically the differences in the "shadowing" pattern induced by valance and sea quarks, neglecting the charm mass effects that are shown to be small below. For isoscalar-corrected ($Z = N = A/2$) target nuclei we average over neutrino- and antineutrino-initiated charged current interactions, $F_i^A(x_B, Q^2) = (F_i^{\nu A}(x_B, Q^2) + F_i^{\bar{\nu}A}(x_B, Q^2))/2$. In the leading-order and leading twist parton model $F_3^A(x_B, Q^2)$ measures the valance quark number density with $\phi_{\mathrm{val.}}(x) \propto x^{-\alpha_{\mathrm{val.}}}$ at small x. $F_2^A(x_B, Q^2)$, a singlet distribution, is proportional to the momentum density of all interacting quark constituents and for $x_B \ll 0.1$ is dominated by the sea contribution, $\phi_{\mathrm{sea}}(x) \propto x^{-\alpha_{\mathrm{sea}}}$. Therefore, the x_B-dependent shift from dynamical nuclear enhanced power corrections, x_{HT} in Eq. (12), generates different modification to $F_2^A(x_B, Q^2)$ and $F_3^A(x_B, Q^2)$. Let $R^{A/A'}_{\mathrm{sea/val.}}(x_B, Q^2)$ be the shadowing ratio determined from nuclei A and A' (for example, ^{56}Fe to ^2D) in F_2 and F_3. If the scale of high twist corrections $\xi^2 \ll Q^2$ [6] and $x_B \leqslant \min(x_A, x_{A'})$, we expand the PDFs to first order in x_{HT} to obtain:

$$R^{A/A'}_{\mathrm{sea/val.}}(x_B, Q^2) = \frac{F_2^A(x_B, Q^2)}{F_2^{A'}(x_B, Q^2)} \Bigg/ \frac{F_3^A(x_B, Q^2)}{F_3^{A'}(x_B, Q^2)} = 1 - (\alpha_{\mathrm{sea}} - \alpha_{\mathrm{val.}})\left(A^{1/3} - A'^{1/3}\right)\xi^2/Q^2 + \cdots. \tag{17}$$

Since $\alpha_{\mathrm{val.}} \approx 0.5$ and $\alpha_{\mathrm{sea}} \approx 1$ vary slowly with Q^2, Eq. (17) predicts a measurable difference in the nuclear shadowing for the structure function F_2 (F_1) in comparison to F_3.

Fig. 3 shows the modification to the DIS structure functions from Eqs. (10)–(16) for large nuclei (^{12}C, ^{56}Fe and ^{208}Pb) relative to the deuteron, calculated with the CTEQ6L parton distribution functions [21]. The bands correspond to a scale for power corrections $\xi^2 = 0.09$–0.12 GeV^2, extracted from the analysis [6] of the NMC and E665 data [7]. The transition $0.01 \leqslant x_B \leqslant 0.1$ region represents the onset of coherent interactions, Eq. (14), and the modest x_B-dependence for $x_B \leqslant 0.01$ is driven by the change in the local slope of the PDFs. The right panels show the Q^2 dependence of the modification from the resummed nuclear-enhanced power corrections, which is noticeably stronger than the DGLAP evolution of leading twist shadowing in the nPDFs [22]. The difference in the suppression pattern of F_2^A and $x_B F_3^A$ in Fig. 3 is qualitatively described by Eq. (17). In contrast, it has been suggested in the framework of a Gluber–Gribov approach [23] that the suppression of the non-singlet distribution may be significantly larger than of the singlet one ($R^{A/A'}_{\mathrm{sea/val.}} > 1$ for $A > A'$). Such distinctly different predictions should be testable in the future ν-factory experiments, for example, at the Fermilab NuMI facility [24].

Although the current $\nu(\bar{\nu}) - A$ DIS measurements are mostly on nuclear targets [25], these data lack the necessary atomic weight systematics to identify small-x_B nuclear shadowing. We do, however, note that our results provide a consistent explanation of the observed small- and moderate-Q^2 power law deviation at small-x_B of the preliminary NuTeV data [11] on $F_2^A(x_B, Q^2)$ and $x_B F_3^A(x_B, Q^2)$ from the next-to-leading order leading twist QCD predictions using MRST parton distribution functions [26].

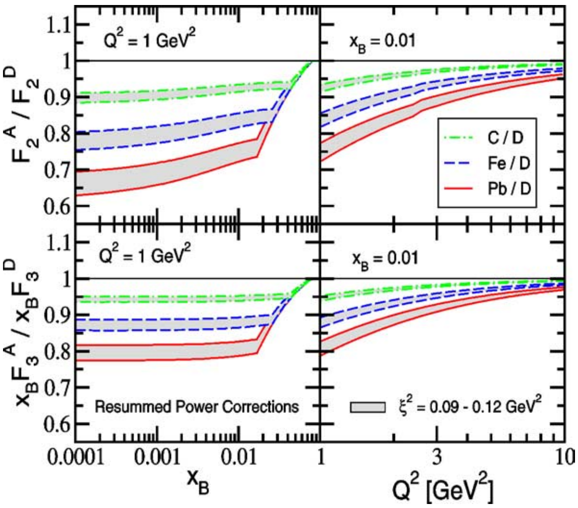

Fig. 3. The predicted nuclear modification for isoscalar-corrected ^{12}C, ^{56}Fe and ^{208}Pb to the neutrino–nucleus DIS stricture functions $F_2^A(x_B, Q^2)$ (top) and $x_B F_3^A(x_B, Q^2)$ (bottom) versus Bjorken x_B (left) and Q^2 (right). The bands correspond to $\xi^2 = 0.09$–0.12 GeV^2 [6].

The latest global QCD fits include $\nu(\bar{\nu}) - A$ DIS data without nuclear correction other than isospin [21]. Such analysis would tend to artificially eliminate most of the higher twist contributions discussed here due to a trade off between the power corrections in a limited range of Q^2 and the shape of the fitted input distributions at Q_0^2, especially within the error bars of current data. An effective way to verify the importance of the nuclear enhanced power corrections for neutrino–nucleus deeply inelastic scattering is via the QCD sum rules, in particular, the Gross–Llewellyn Smith (GLS) sum rule [8]

$$S_{\mathrm{GLS}} = \int_0^1 dx_B \, \frac{1}{2x_B}\left(x_B F_3^{\nu A} + x_B F_3^{\bar{\nu} A}\right). \tag{18}$$

At tree level Eq. (18) counts the number of valance quarks in a nucleon, $S_{\mathrm{GLS}} = 3$. Since valence quark number conservation is enforced in the extraction of twist-2 nucleon/nucleus PDFs, the adjustments of input parton distributions can alter their shape but not the numerical contributions to the GLS sum rule.

The effect of scaling violations can modify S_{GLS}, and at $\mathcal{O}(\alpha_s)$ [9]

$$\Delta_{\mathrm{GLS}} \equiv \frac{1}{3}(3 - S_{\mathrm{GLS}}) = \frac{\alpha_s(Q^2)}{\pi} + \frac{\mathcal{G}}{Q^2} + \mathcal{O}\left(Q^{-4}\right). \tag{19}$$

Loop contributions to the GLS sum rule are known to $\mathcal{O}(\alpha_s^3)$ [27]. Although power corrections can also modify the shape of *nucleon* structure functions, recent precision DIS data on both hydrogen and deuterium targets from JLab [28] indicate that effects from higher twist to the lower moments of structure functions are very small at Q^2 as low as 0.5 GeV^2, which confirms the Bloom–Gilman duality [29]. A recent phenomenological study [30] also suggests that power corrections to the proton $F_2(x_B, Q^2)$ have different sign in the small- and large-x_B regions and largely cancel in the QCD sum rules.

On the other hand, the coherence between different nucleons inside a large nucleus is only relevant for $x_B \leqslant x_N$. The suppression of structure functions at small Bjorken x_B in Fig. 3, caused by the nuclear enhanced dynamical power corrections, cannot be canceled in the moments and further reduces the numerical value of S_{GLS}. Fig. 4 shows a calculation of Δ_{GLS} from Eqs. (10) and (11) for ^{56}Fe. While the effect of charm mass is seen to be small relative to α_s/π, for $Q^2 \sim 1$ GeV^2 nuclear enhanced higher twists may contribute as much as $\sim 10\%$ to Δ_{GLS}.

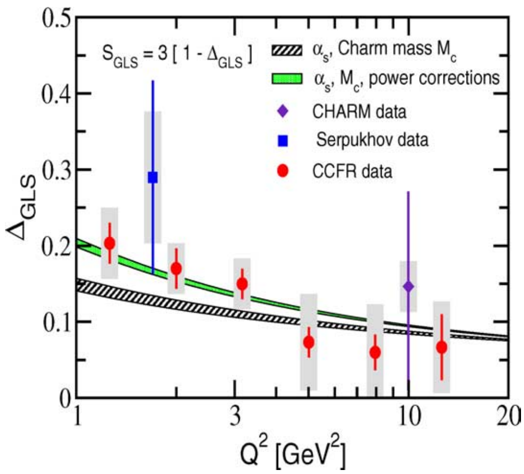

Fig. 4. Δ_{GLS} calculated to $\mathcal{O}(\alpha_s)$ with charm mass ($M_c = 1.35$ GeV) effects (stripes) and $M_c +$ resummed power corrections (band). Data is from CCFR, CHARM and IHEP-JINR [10].

Their Q^2 behavior is consistent with the trend in the current data [10]. For comparison, we found no deviations for this sum rule induced by the EKS98 scale dependent parameterization of nuclear effects [22], which is again a consequence of the valance quark number conservation in leading twist shadowing.

5. Implications for extraction of $\sin^2\theta_W$

Based on a comparison of charged and neutral current neutrino interactions (separated on the basis of event topology) with an iron-rich heavy target, the NuTeV Collaboration reported a measurement of

$$\sin^2\theta_W^{(\text{on-shell})} = 0.2277 \pm 0.0013(\text{stat.}) \pm 0.0009(\text{syst.}),$$

neglecting the very small top quark and Higgs mass corrections. This result is approximately 3 standard deviations [1] above the Standard Model (SM) expectation value $\sin^2\theta_W = 0.2227 \pm 0.0004$. The NuTeV's result was derived from a quantity that is a close approximation to the Paschos-Wolfenstein relationship

$$R^- = \frac{\sigma^{\text{NC}}(\nu) - \sigma^{\text{NC}}(\bar{\nu})}{\sigma^{\text{CC}}(\nu) - \sigma^{\text{CC}}(\bar{\nu})} \approx \frac{1}{2} - \sin^2\theta_W. \tag{20}$$

Corrections to Eq. (20) include higher order and non-perturbative QCD effects, higher order electroweak effects and nuclear effects. Based on a QCD global analysis of parton structure, Kretzer et al. argue [31] that the uncertainties in the theory which relates R^- to $\sin^2\theta_W$ are substantial on the scale of the precision NuTeV data and suggest that the $\sin^2\theta_W$ measurement, NuTeV dimuon data and other global data sets used in QCD parton structure analysis can all be consistent within the SM.

Because a heavy target was used, several nuclear effects can enter the cross sections to influence the extraction of $\sin^2\theta_W$ [32]. Since nuclear enhanced power corrections were not included in NuTeV's analysis, Miller and Thomas pointed out that nuclear shadowing from a vector meson dominance (VMD) model could affect the charged and neutral current neutrino scattering differently, and therefore change the predictions for the ratios of neutral current (NC) over charged current (CC) cross sections, $R^{\nu(\bar{\nu})} = \sigma^{\text{NC}}(\nu(\bar{\nu}))/\sigma^{\text{CC}}(\nu(\bar{\nu}))$, and the extraction of $\sin^2\theta_W$ [2]. The NuTeV Collaboration argued [3,32] that such possibility was considered unlikely because R^- has little sensitivity to process-dependent nuclear effects.

In this Letter we calculated the process-dependent nuclear effects in the neutrino–nucleus *differential* cross sections, Eq. (1), in the *perturbatively accessible* DIS region. Our predictions on the nuclear modification to the $\nu(\bar{\nu})$-A structure functions in Fig. 3 should be relevant for Q^2 between 1 and 10 GeV^2. While for the mean $\langle Q^2\rangle_\nu = 25.6$ GeV^2 and $\langle Q^2\rangle_{\bar{\nu}} = 15.4$ GeV^2 the effect of dynamical power corrections is small, a large fraction of the final data sample cover the $x_B < 0.1$, $Q^2 < 10$ GeV^2 range where shadowing can be as large as $\sim 20\%$. We note that the NuTeV measurement constitutes a $\sim 2\%$ *increase* in the value of $\sin^2\theta_W$ relative to the SM, or equivalently $\sim 4\%$ *reduction* of the expected total neutrino–nucleus cross section. Including shadowing into the expected total cross sections will certainly reduce the discrepancy of $\sin^2\theta_W$. However, without knowing the nuclear enhanced power corrections to the structure functions at $Q^2 < 1$ GeV^2, and the detailed Monte Carlo simulation of event distributions, it is difficult to estimate the precise corrections to the extraction of $\sin^2\theta_W$. We, nevertheless, note that at small Bjorken x_B, the calculated nuclear structure functions $F_2^A(x_B, Q^2)$ and $F_3^A(x_B, Q^2)$ in neutrino-iron DIS qualitatively describe the low-x_B and low-Q^2 suppression trend in the preliminary data, presented by the NuTeV Collaboration at DIS 2003 [11].

6. Conclusions

In the framework of the perturbative QCD collinear factorization approach [33,34], we computed and resumed the tree level perturbative expansion of nuclear enhanced power corrections to the structure functions measured in inclusive (anti)neutrino–nucleus deeply inelastic scattering. We demonstrated that these corrections commute with the final state heavy quark effects and identified the new contributions to the longitudinal structure function $F_L^A(x_B, Q^2)$. Our calculated Q^2-dependent modification to the Gross–Llewellyn Smith sum rule agrees well with the existing measurements on an iron target [10]. Our approach predicts a non-negligible difference in the small-x_B shadowing of the structure functions $F_2^A(x_B, Q^2)$ ($F_1^A(x_B, Q^2)$) and $F_3^A(x_B, Q^2)$, which is consistent with the trend in the preliminary NuTeV data [11]. Although our results, valid in the perturbative region, are unlikely to have an immediate impact on the NuTeV's extraction of $\sin^2\theta_W$, the predicted x_B-, Q^2-, and A-dependence of the structure functions in the shadowing region can be tested at the future Fermilab NuMI facility [24].

Acknowledgements

This work is supported in part by the US Department of Energy under Grant No. DE-FG02-87ER40371. We thank G. Zeller, J. Morfin, G. Sterman and E. Shuryak for useful discussion.

References

[1] G.P. Zeller, et al., Phys. Rev. Lett. 88 (2002) 091802;
G.P. Zeller, et al., Phys. Rev. Lett. 90 (2003) 239902, Erratum.
[2] G.A. Miller, A.W. Thomas, hep-ex/0204007.
[3] G.P. Zeller, et al., NuTeV Collaboration, hep-ex/0207052.
[4] J.W. Qiu, G. Sterman, Int. J. Mod. Phys. E 12 (2003) 149, references therein.
[5] J.W. Qiu, Nucl. Phys. A 715 (2003) 309, and references therein.
[6] J.W. Qiu, I. Vitev, hep-ph/0309094.
[7] M. Arneodo, et al., Nucl. Phys. B 441 (1995) 12;
P. Amaudruz, et al., Nucl. Phys. B 441 (1995) 3;
M.R. Adams, et al., Z. Phys. C 67 (1995) 403;
M.R. Adams, et al., Phys. Rev. Lett. 68 (1992) 3266.
[8] D.J. Gross, C.H. Llewellyn Smith, Nucl. Phys. B 14 (1969) 337.
[9] R. Brock, et al., Rev. Mod. Phys. 67 (1995) 157.

[10] J.H. Kim, et al., Phys. Rev. Lett. 81 (1998) 3595;
F. Bergsma, et al., Phys. Lett. B 123 (1983) 269;
L.S. Barabash, et al., hep-ex/9611012.
[11] D. Naples, et al., hep-ex/0307005.
[12] H. Georgi, H.D. Politzer, Phys. Rev. D 14 (1976) 1829.
[13] A.H. Mueller, Nucl. Phys. B 558 (1999) 285, references therein.
[14] R.M. Barnett, Phys. Rev. D 14 (1976) 70.
[15] X.F. Guo, J.W. Qiu, W. Zhu, Phys. Lett. B 523 (2001) 88.
[16] J.W. Qiu, Phys. Rev. D 42 (1990) 30.
[17] E.V. Shuryak, A.I. Vainshtein, Nucl. Phys. B 201 (1982) 141.
[18] J.W. Qiu, I. Vitev, Phys. Lett. B 570 (2003) 161;
M. Gyulassy, P. Levai, I. Vitev, Phys. Rev. D 66 (2002) 014005;
M. Gyulassy, P. Levai, I. Vitev, Nucl. Phys. B 594 (2001) 371.
[19] N. Cabibbo, Phys. Rev. Lett. 10 (1963) 531.
[20] J.W. Qiu, Nucl. Phys. B 291 (1987) 746.
[21] J. Pumplin, et al., JHEP 0207 (2002) 012.
[22] K.J. Eskola, V.J. Kolhinen, C.A. Salgado, Eur. Phys. J. C 9 (1999) 61.
[23] S.A. Kulagin, hep-ph/9809219.
[24] J.G. Morfin, J. Phys. G 29 (2003) 1935;
M.L. Mangano, et al., hep-ph/0105155, references therein.
[25] U.K. Yang, et al., Phys. Rev. Lett. 87 (2001) 251802;
S.I. Alekhin, et al., Phys. Lett. B 512 (2001) 25.
[26] R.S. Thorne, R.G. Roberts, Phys. Lett. B 421 (1998) 303.
[27] I. Hinchliffe, A. Kwiatkowski, Annu. Rev. Nucl. Part. Sci. 46 (1996) 609.
[28] I. Niculescu, et al., Phys. Rev. Lett. 85 (2000) 1182.
[29] E.D. Bloom, F.J. Gilman, Phys. Rev. Lett. 16 (1970) 1140;
E.D. Bloom, F.J. Gilman, Phys. Rev. D 4 (1971) 2901.
[30] S. Alekhin, Phys. Rev. D 68 (2003) 014002.
[31] S. Kretzer, F. Olness, J. Pumplin, M.H. Reno, D. Stump, W.K. Tung, hep-ph/0312322, and references therein.
[32] K.S. McFarland, et al., Nucl. Phys. B (Proc. Suppl.) 112 (2002) 226.
[33] J.C. Collins, D.E. Soper, G. Sterman, Adv. Ser. Dir. High Energy Phys. 5 (1988) 1.
[34] J.W. Qiu, G. Sterman, Nucl. Phys. B 353 (1991) 137.